Self-assembled complete hair follicle organoids by coculture of neonatal mouse epidermal cells and dermal cells in Matrigel

Sitian Xie[1]^, Liyun Chen[1], Mingjun Zhang[1], Cuiping Zhang[2], Haihong Li[1,3]

[1]Department of Plastic Surgery and Burn Center, The Second Affiliated Hospital, Shantou University Medical College, Shantou, China; [2]Wound Healing and Cell Biology Laboratory, The First Affiliated Hospital, Chinese PLA General Hospital, Beijing, China; [3]Department of Wound Repair, Institute of Wound Repair and Regeneration Medicine, Southern University of Science and Technology Hospital, Southern University of Science and Technology School of Medicine, Shenzhen, China

Contributions: (I) Conception and design: C Zhang; (II) Administrative support: H Li; (III) Provision of study materials or patients: L Chen; (IV) Collection and assembly of data: S Xie; (V) Data analysis and interpretation: M Zhang; (VI) Manuscript writing: All authors; (VII) Final approval of manuscript: All authors.

Correspondence to: Haihong Li, MD. Professor, Department of Plastic Surgery and Burn Center, The Second Affiliated Hospital, Shantou University Medical College, North Dongxia Road, Shantou 515041, China; Department of Wound Repair, Institute of Wound Repair and Regeneration Medicine, Southern University of Science and Technology Hospital, Southern University of Science and Technology School of Medicine, Shenzhen 518055, China. Email: lihaihong1051@126.com; Cuiping Zhang. Professor, Wound Healing and Cell Biology Laboratory, The First Affiliated Hospital, Chinese PLA General Hospital, 51 Fucheng Road, Beijing 100048, China. Email: zcp666666@sohu.com.

Background: 3D organoid cultures of hair follicles (HFs) are powerful models that mimic native HF for both in-depth study of HF disease and precision therapy. However, few studies have investigated the complete structure and properties of HF organoids. To investigate and characterize the complete HF organoids self-assembled by coculture of neonatal mouse epidermal cells (MECs) and dermal cells in Matrigel.

Methods: Fresh epidermal and dermal cells from newborn mice (n=4) were isolated, and cocultured (1:1 ratio) in Matrigel using DMEM/F12 medium for 1 week. During the culture, an inverted microscope was used to observe the morphology of the 3D constructs. After 1 week, hematoxylin-eosin (HE) and immunofluorescence (IF) staining of HF-related markers (K5, K73, AE13, and K10), HF stem cell markers (K15, CD34, CD49f), skin-derived precursor-related marker (Nestin), and dermal papillae (DP)-specific markers (SOX2 and ALP) was performed in the harvested constructs to identify the HF organoids.

Results: Epidermal and dermal cells self-assembled into HF organoids comprising an infundibular cyst-like structure, a lower segment-like structure, and a bulb-like structure from tail to root. The HF organoid had multiple, well-defined compartments similar to native anagen HF. Of the three segments, K73 was expressed in the inner root sheath-like layer, AE13 was localized in the hair shaft-like structure, K5, K15, CD34, and CD49f were present in the outer root sheath-like layer, Nestin labeled the connective tissue sheath-like layer, and SOX2 and ALP were expressed in the DP-like structure. Furthermore, K10 and K73 were expressed in the infundibular cyst-like structure. The expression of these molecular proteins was consistent with native anagen HF.

Conclusions: The complete HF organoid regenerated in Matrigel has specific compartments and is an excellent model to study HF disease and precision therapy.

Keywords: 3D culture; hair follicles (HFs); Matrigel; organoids; precision therapy

Submitted Jun 01, 2022. Accepted for publication Jul 08, 2022.
doi: 10.21037/atm-22-3252
View this article at: https://dx.doi.org/10.21037/atm-22-3252

^ ORCID: 0000-0003-2846-5128.

Introduction

A unique phenomenon of human evolution is the loss of most of the body hair. Hair is only present in limited areas, such as the scalp, genital area, armpits, and face, but that little bit of hair is of immeasurable importance. Diseases in the quantity or quality of hair, such as hair loss, are linked to body image and self-esteem, and have a huge effect on behavior and personal well-being, so the importance of hair cannot be overemphasized.

Epithelial-mesenchymal interactions play an important role in hair development and cycling (1). Embryologically, hair placodes originate from epidermal basal cells, which then project downward and elongate into epithelial cords under the influence of the condensed mesenchyme of the underlying dermis. The epithelial cords and the dermal mesenchymal condensate eventually mature into complete integral hair follicles (HFs) (2). The dynamic and alternating changes of numerous molecular signals are the underlying mechanisms of HF morphogenesis. HF cycle includes anagen (growth phase), catagen (regression phase) and telogen (resting phase) under the regulation of several signaling pathways, including Wnt/β-catenin, FGF, Shh, and Notch. For instance, Wnt/β-catenin activation and BMP suppression in the HF initiates the anagen induction, and BMP activation induces the telogen (3).

The HF can be anatomically and functionally divided into two distinct segments: the upper segment (which includes the infundibulum and the isthmus) and the lower segment (which includes the bulb). The differences between the two segments are that the upper segment is very stable and unaffected by the maturation and shedding of the hair, and the lower segment is actively involved in hair growth and undergoes considerable morphological change according to different hair cycles (4). The boundary between the two segments of the HF is the bulge, where the arrector pili muscle inserts. The center of the bulb has an inward depression, that is, a dermal papillae (DP).

Hair loss, also known as alopecia or baldness, is a common health issue that affects more than 50% of the global population (5). Although there is excellent research on the homeostasis and regeneration of HFs, there is still no good solution to the problem of hair loss.

Three-dimensional (3D) organoid cultures are powerful models of native tissues and organs for in-depth study of both disease and precision therapy. Recent advances in 3D organoid culture technologies have resulted in the generation of various mini-organs that resemble the tissues of their origin (6). In the field of hair regeneration, organoid manipulation technology has made rapid progress. The development of HF organoids is focused on for the approaches for HF disease modeling, tissue engineering, drug development, diagnosis, and regenerative medicine. However, it is challenged by low efficiency and high cost. Lei *et al.* showed that mouse neonatal epidermis and dermis cells self-organized into planar hair-bearing skin via an early organoid-like aggregation state using a 3D droplet culture method (7). Lee *et al.* reported that *de novo* HFs generated from mouse embryonic stem cells could serve as a model of skin development that mimics the process of embryonic folliculogenesis (8). The same team co-induced epidermal keratinocytes and mesenchymal tissues from human induced pluripotent stem cells and gave rise to complex organoids containing hairy skin and appendages that recapitulate second-trimester human tissue through a complex protocol during an incubation period of 4–5 months (9). These studies are considered landmark studies focused on hair regeneration (10).

HF organoids could be regenerated from stem cells or progenitor cells. In previous studies, in *in vitro* Matrigel culture, HF organoids were described as HF-derived organoids (11), aggregates (12), and 3D spheroids (13). They had a similar characterization, that is, the organoids were round, densely cellular structures with a neopapilla or a keratinized center. While *in vitro* droplet culture, another *in vitro* culture method, hair peg-like structures were formed (14). Furthermore, in pluripotent stem cell induction studies, hair follicles were produced that grew radially outward the hair-bearing skin organoids (8,9). However, despite the promise of HF organoid research, few studies have investigated the complete structure and properties of HF organoids. In this study we aimed to comprehensively investigate the characterization of self-assembled HF organoids by coculturing neonatal mouse epidermal and dermal cells in Matrigel, which included detecting the complete structure, the specific marker protein expressions, and the location of stem cells in various segments of the HF organoid. We present the following article in accordance with the ARRIVE reporting checklist (available at https://atm.amegroups.com/article/view/10.21037/atm-22-3252/rc).

Methods

Animals

Newborn C57BL/6J mice (male, day 0) and 4–6-week-old

male C57BL/6J mice were purchased from the Shantou University Medical College Laboratory Animal Center. The mice were housed under a 12-h light/dark cycle with food and water *ad libitum*, and allowed to acclimate for 1 week. All animal-related procedures were approved by the Ethics Committee of Shantou University Medical College (Shantou, China) (No. SUMC2019-217), in compliance with the institutional guidelines for the care and use of animals. A protocol was prepared before the study without registration.

Preparation of newborn mouse dermal and epidermal cells

Mouse epidermal cells (MECs) and mouse dermal cells (MDCs) were obtained from the skin of the newborn C57BL/6J mice (n=4) on Day 0 as described previously (15). Briefly, after the mice were killed humanely by cervical dislocation, the full-thickness dorsal skin was scraped off the subcutaneous fat and cut into small strips, which were incubated overnight in 0.1% (wt/vol) dispase solution (D4693, Sigma, USA) at 4 ℃, washed three times in phosphate-buffered saline, and split into the epidermis and dermis with forceps, before mincing. The epidermis was incubated in 0.25% (wt/vol) trypsin-ethylenediaminetetraacetic acid (EDTA) (25300054, Invitrogen, USA) at 37 ℃ for 10 min, whereas the dermis was incubated in 0.2% (wt/vol) collagenase (17101-015, Invitrogen) at 37 ℃ for 1 h. After digestion, each component was filtered sequentially through 100- and 40-μm mesh cell strainers. Cells were collected by centrifugation at 300 g for 5 min and resuspended in DMEM (C11995500BT, Invitrogen) for cell grafting.

In vitro 3D organoid regeneration in Matrigel

Suspensions of 2×10^6 MECs and 2×10^6 MDCs in 500 μL DMEM were added to 0.5 mL cold Matrigel basement membrane matrix (354248, BD Biosciences, USA), mixed with cooled pipettes, and then added to the wells of a 6-well Costar culture plate (3516, Corning, USA). The plates were incubated at 37 ℃ for 30 min to allow gel formation, and then DMEM/F12 medium containing penicillin/streptomycin (15140122, Pen/Strep; 10,000 U/mL; 1%; Gibco/Thermo Fisher Scientific), 2 nmol/mL triiodothyronine, 0.4 μg/mL hemisuccinate hydrocortisone, 1% insulin-transferrin-selenium, 10 ng/mL human EGF recombinant protein, and 2% fetal bovine serum were added. The medium was subsequently changed every other day. The 3D constructs were observed under an inverted microscope (Olympus, Japan) and the experiment was repeated three times.

Hematoxylin-eosin (HE) and immunofluorescence (IF) staining of paraffin-embedded organoids and dorsal skin

On the 7th day of culture, the medium was aspirated, 4% formaldehyde was added to the 6-well plate, the Matrigel was gently disrupted, transferred to a centrifuge tube, placed on ice for fixation overnight, and spun down at 300 g for 5 min. The precipitate was wrapped with microscope glass cleaning paper to be embedded in paraffin. Three of the 4–6-week-old male C57BL/6J mice were killed humanely by cervical dislocation and their dorsal skins were fixed overnight in 4% paraformaldehyde. After that, the precipitate and skin were embedded in paraffin respectively, and were cut into 5-μm-thick sections for conventional HE and IF staining.

IF staining was performed as previously reported (16). The primary antibodies used were rabbit anti-K5 (1:200, ab52635), rabbit anti-K10 (1:500, ab76318), rabbit anti-K73 (1:150, ab181383), Mouse anti-AE13 (1:200, ab16113), rabbit anti-K15 (1:500, ab52816), rabbit anti-CD34 (1:250, ab81289), rabbit anti-CD49f (1:500, ab181551), mouse anti-Nestin (1:500, ab6142), rabbit anti-SOX2 (1:100, ab92494), and rabbit anti-ALP (1:500, ab108337). All antibodies were purchased from Abcam (UK). The secondary antibodies were a Cy3-labeled goat anti-rabbit IgG (H + L) (A0516, Beyotime, China) for the rabbit antibodies and an Alexa Fluor 488-labeled goat anti-mouse IgG (H + L) (A0428, Beyotime) for the mouse antibodies. Nuclei were counterstained with 4',6-diamidino-2-phenylindole (DAPI; Beyotime). Sections omitting the primary antibodies were used as negative controls. Sections were viewed with a fluorescence microscope (Olympus BX51, Japan). All the primary antibodies used were validated for fluorescence immunohistochemistry on formalin-fixed tissues. HE and IF staining were performed once for each 3D construct, and repeated three times for three constructs.

Results

Regeneration of 3D organoids of HFs from isolated newborn mouse epidermal and dermal cells

The growing organoids were observed by bright-field microscopy. After being suspended in Matrigel, the

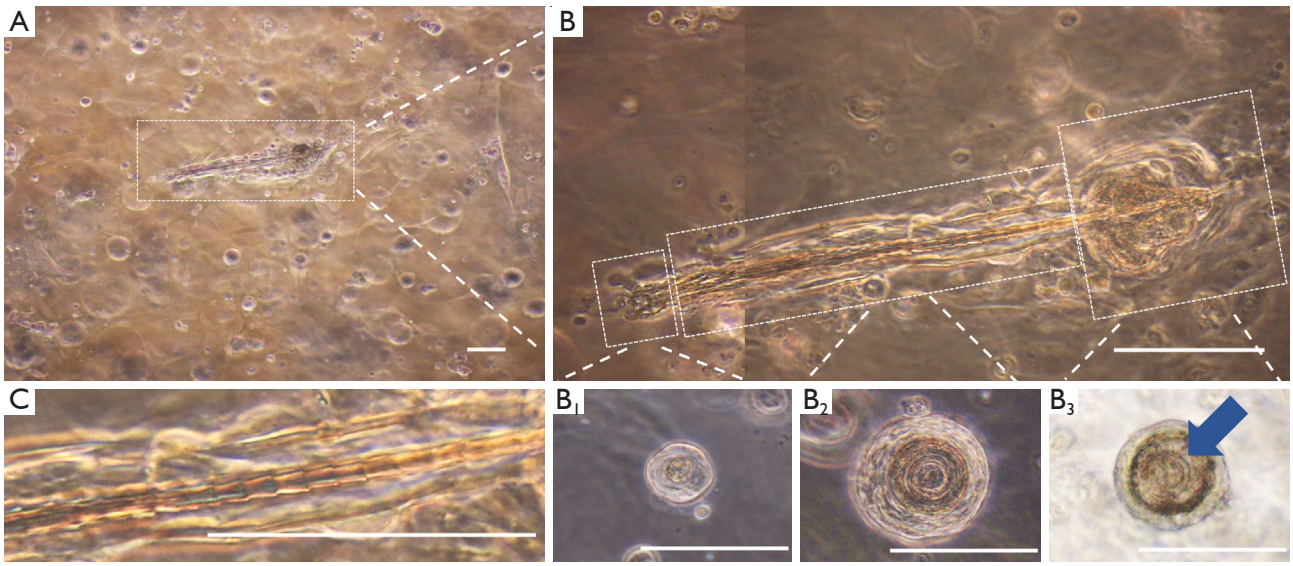

Figure 1 HF organoid culture and characterization under light microscopy. (A) Microscopic image of organoid reconstruction in Matrigel. (B) Magnified longitudinal view of HF organoid. (B_1-B_3) Cross-sections of bulb-like structure, lower segment-like structure, and infundibular cyst-like structure, respectively. (C) Magnification of hair shaft in the HF organoid, showing the orientation of the cuticular scales. Blue arrow shows a hair shaft. All scale bars =50 μm. HF, hair follicle.

dissociated dermal and epidermal cells started to grow through continuous cell division. A large number of hair peg-like structures containing bulb-like, stem-like, and cyst-like structures were found in the Matrigel on day 7 (*Figure 1A*,*1B*).

According to the results and corresponding to the structure of native anagen HF, these structures of the HF organoid were called the bulb-like structure, lower segment-like structure, and infundibular cyst-like structure. The cuticular scales covering the hair shaft were found to be pointed from the stem to the cyst-like structure (*Figure 1C*). The infundibular cyst-like structure was on the tail-tip of the hair peg-like structures (i.e., HF organoids). The bulb-like structure was small, spherical, and dense. The hair shaft was located in the center of the lower segment-like structure and surrounded by a multilayered structure. The infundibular cyst-like structure was irregularly vesicularized and the hair shaft grew into it. The multilayered structure of the wall was looser than that of the lower segment-like structure.

We also observed abundant circular structures (i.e., cross-sections of organoids), which were divided into three types. According to the spatial position of the organoids in the Matrigel, we classified the structures into three cross-sections of the different segments of HF organoid. The bulb-like structure of the HF organoid was small with a dense cellular cluster in the center (*Figure 1B$_1$*). The lower segment-like structure comprised external and internal concentric circles with a complex multilayered configuration (*Figure 1B$_2$*), similar to the structure of the cross-section of the native HF lower segment including the medulla, cortex of the hair shaft, inner root sheath (IRS), and outer root sheath (ORS). The infundibular cyst-like structure was rounded, and the hair shaft was visible within the internal structure (*Figure 1B$_3$*).

HF organoid compartments in longitudinal section

HE staining revealed that the longitudinal section of the HF organoid comprised the ORS, IRS, hair shaft, and DP, which was shown in the schematic illustration (*Figure 2A*), as similar to that of a native HF (*Figure 2B*). According to the morphology of the longitudinal- and cross-sections of the various segments of the HF organoid observed by bright-field microscopy and HE staining, we divided the HF organoid from tail end to root into three segments: infundibular cyst-like structure, lower segment-like structure, and bulb-like structure. The results of HE staining and IF staining for HF-related markers (K5, K73, AE13, and K10), HF stem cell markers (K15, CD34,

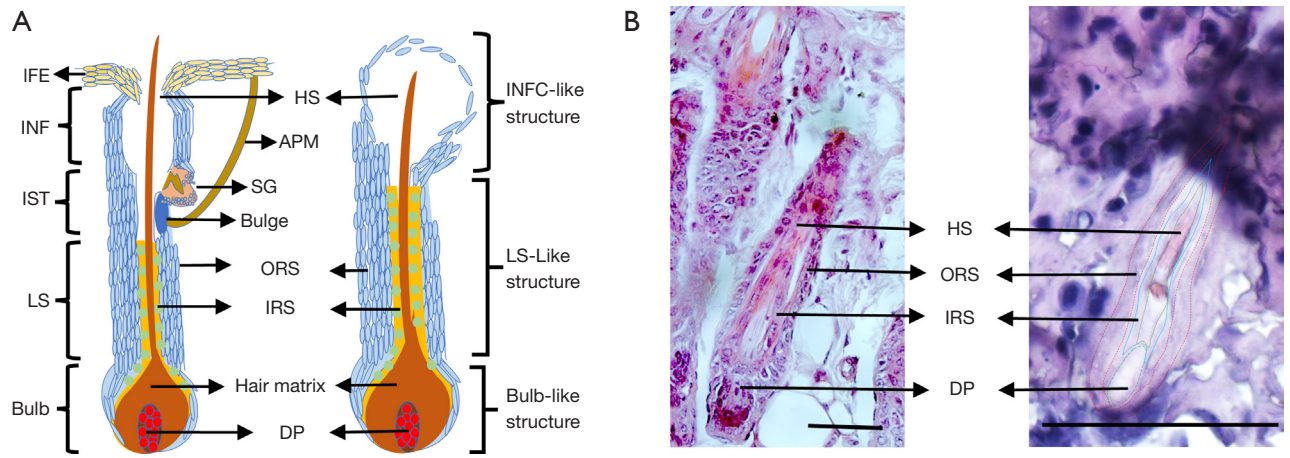

Figure 2 Comparison of compartments in longitudinal section between native HF and HF organoid. (A) Schematic illustrations of the compartments in longitudinal section of native HF and HF organoid. The HF is divided into the INF, IST, LS, and bulb. The HF organoid is divided into the INFC-like structure, LS-like structure, and bulb-like structure. (B) HF organoid has a similar structural composition as the native HF under HE staining. The basic units are HS, IRS, ORS, and DP. All scale bars =50 μm. IFE, interfollicular epidermis; INF, infundibulum; IST, isthmus; LS, lower segment; HS, hair shaft; APM, arrector pili muscle; SG, sebaceous gland; ORS, outer root sheath; IRS, inner root sheath; DP, dermal papillae; INFC-like, infundibulum cyst-like; LS-like, lower segment-like; HF, hair follicle; HE, hematoxylin-eosin.

Table 1 Localization of antigen expression in HF organoid and native HF

Antigen	HF organoid			Native HF		
	Bulb-like structure	Lower segment-like structure	Infundibular cyst-like structure	Bulb	Lower segment	Infundibulum
K5	+	+	+	+	+	+
K73	+	+	+	+	+	+
AE13	–	+	+	–	+	+
K10	–	–	+	–	–	+
K15	+	+	+	+	+	+
CD34	+	+	+	+	+	+
CD49f	+	+	+	+	+	+
Nestin	+	–	–	+	–	–
SOX2	+	–	–	+	–	–
ALP	+	–	–	+	–	–

+, expressed; –, not expressed. HF, hair follicle.

CD49f), skin-derived precursor-related marker (Nestin), and DP-specific markers (SOX2 and ALP) of various segments were compared with those of the corresponding segments of native HFs (*Table 1*).

Comparison of the cytoarchitecture and molecular markers of the infundibular cyst-like structure of the HF organoid and infundibulum of the native HF

HE staining showed an oval cross-section of the

infundibulum of the native HF, consisting of ≈2 layers of cells, with a rounded cross-section of the hair shaft inside. The infundibular cyst-like structure of HF organoid was similar to that of the infundibulum (*Figure 3*). The cross-section of the infundibular cyst-like structure had a loose, circular cytoarchitecture with 1–2 layers of cells (equivalent to the ORS), containing a round core of keratin (equivalent to the hair shaft).

The infundibular cyst-like structure of the HF organoid expressed HF-related markers (K5, K73, AE13, K10) and HF stem cell-related markers (K15, CD34, CD49f). Moreover, K5, K10, and K73 were slightly expressed in the cells of the circular cytoarchitecture but strongly localized in the inner layer. K15, CD34, and CD49f were unevenly localized in the cells of the circular cytoarchitecture. AE13 was present at the center (equivalent to the hair shaft). In the infundibulum of the native HF, K5 staining was prominent in the cells of the ORS. The cellular localization of K10, K73, AE13, K15, CD34 and CD49f was similar to that found in the infundibular cyst-like structure of the HF organoid. The DP-specific markers (SOX2, ALP) and skin-derived precursor-related marker (Nestin) were not detected in either the infundibular cyst-like structure or the infundibulum of the native HF. Therefore, the infundibular cyst-like structure of the HF organoid was considered to be equivalent to the infundibulum of HFs.

Comparison of the lower segment-like structure of the HF organoid with the lower segment of the native HF

HE staining revealed the cross-section of the lower segment-like structure of the HF organoid was composed of a concentric circular, densely stratified cellular structure with more than 3 layers (equivalent to the ORS) with a keratinized center (equivalent to the hair shaft) (*Figure 4*). An IRS-like structure was obviously located between the ORS-like and hair shaft-like structures. The morphology was similar to that of the lower segment of native HF.

IF staining showed that all lower segment-like structures of the HF organoid expressed HF-related markers (K5, K73, AE13) and HF stem cell-related markers (K15, CD34, CD49f), but was negative for K10, Nestin, SOX2, and ALP. K5, K15, CD34, and CD49f were expressed in the outer layer (equivalent to the ORS), in which K5 staining was prominent, K15 labeling was uneven, and CD34 and CD49f were present in the periphery. K73 was strongly localized in the inner layer (equivalent to the IRS). AE13 was expressed in the center (equivalent to the hair shaft). The expressions of molecular markers in the lower segment-like structure were similar to those of the lower segment of HFs.

Comparison of the bulb-like structure of the HF organoid with the bulb of the native HF

HE staining demonstrated that the core of the bulb-like structure of the HF organoid (equivalent to the DP) was composed of a compact mass of cells with larger nuclei (*Figure 5*). IRS-like and hair matrix-like layers could be vaguely distinguished between the ORS-like and DP-like structures in the upper bulb, and the lower bulb had no obvious IRS-like layer (data not shown). The bulb of the native HF had a similar morphology to the bulb-like structure.

IF staining showed that HF-related markers (K5, K73), HF stem cell-related markers (K15, CD34, CD49f), SKP-related markers (Nestin), and DP-specific markers (SOX2, ALP) were expressed in the bulb-like structure. AE13 and K10 were not detected. Moreover, K5, K15, CD34, and CD49f were expressed in the outer layer of the bulb-like structure (equivalent to the ORS). K73 was strongly localized in the inner layer (equivalent to the IRS). Nestin was expressed in the cells immediately adjacent to the bulb-like structure (equivalent to the connective tissue sheath). SOX2 and ALP were expressed in the core of the bulb-like structure (equivalent to the DP). The expressions of these markers in the bulb-like structure were similar to those in the bulb of native HF, which showed that the regenerated bulb-like structure had the same properties as the *in vivo* bulb.

Discussion

Complete HF organoids, self-assembled by coculture of neonatal MECs and MDCs in Matrigel, comprised an infundibular cyst-like structure, lower segment-like structure, and bulb-like structure from tail to root. Different segments displayed similar characterization to the corresponding segment of native HFs in both cytoarchitecture and molecular markers. Owing to this HF organoid model is in an environment that simulates endogenous cell tissue and organ structure, it provides a very representative *in vitro* model for the researches on HF biology, mechanism of HF disease occurrence and development, drug screening, and personalized treatment.

The HF begins at the surface of the epidermis, resides in the dermal layer, and is made up of hair papillae, hair

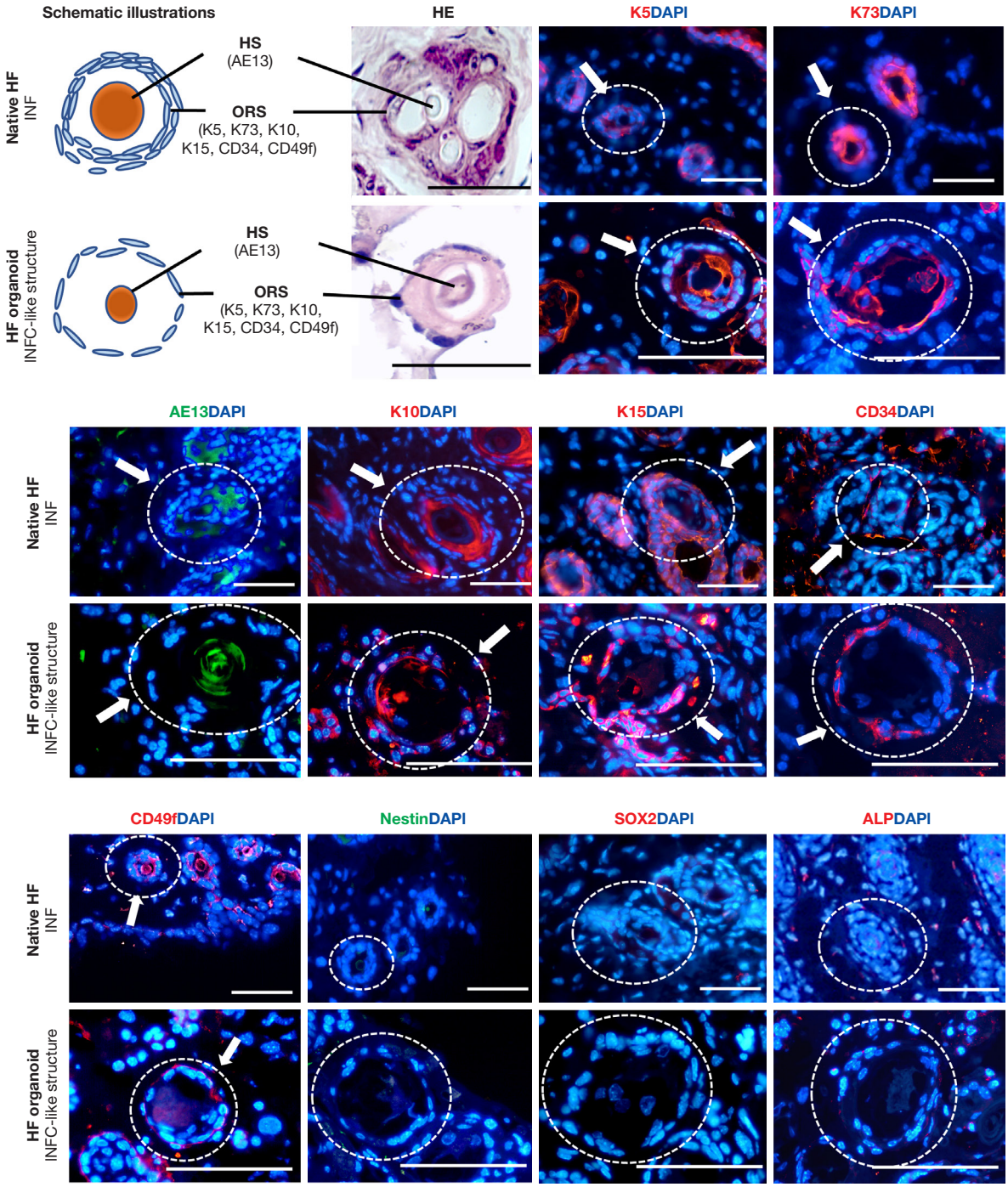

Figure 3 HE staining and expressions of HF-related markers, HF stem cell-related markers, and skin-derived precursor-related markers by IF staining in the infundibulum of the native HF and the infundibular cyst-like structure of the HF organoid. The morphology and marker expressions of the infundibular cyst-like structure of the HF organoid are similar to those of the infundibulum of the native HF in the cross-section, as shown in the schematic illustrations (top left). For both structures, the HF-related markers (K5, K73, and K10) and the HF stem cell-related markers (K15, CD34, CD49f) are present at the ORS (outer root sheath), and AE13 labels the HS (hair shaft). The dermal papillae-specific markers (SOX2, ALP) and skin-derived precursor-related marker (Nestin) are not detected. Dashed lines encircle the target structures for analysis. White arrows show the marker expression sites. All scale bars =50 μm. HF, hair follicle; INF, infundibulum; INF-like structure, infundibular cyst-like structure; HS, hair shaft; ORS, outer root sheath; HE, hematoxylin-eosin.

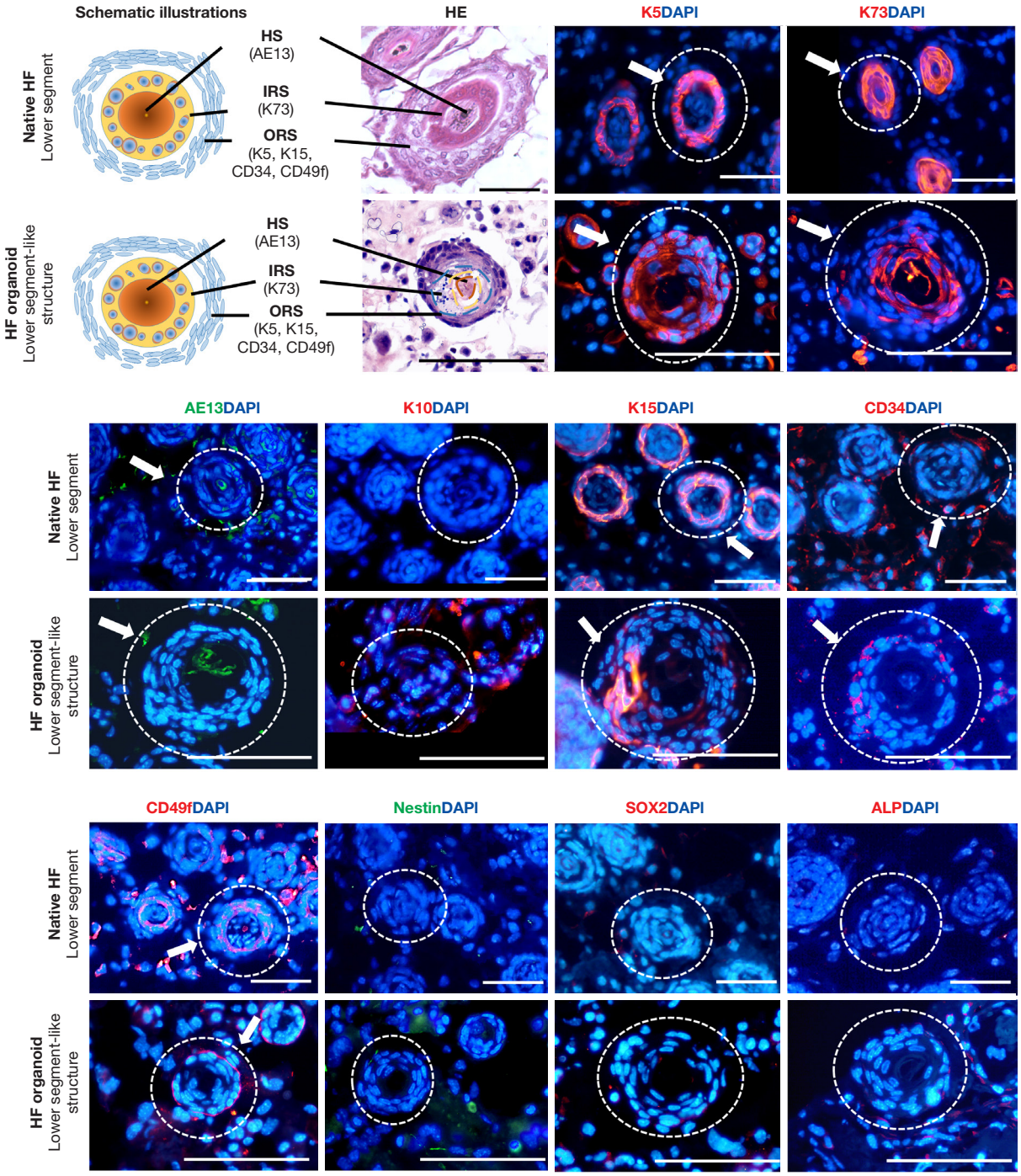

Figure 4 HE staining and expressions of HF-related markers, HF stem cell-related markers, and skin-derived precursor-related markers by IF staining in the lower segment of the native HF and the lower segment-like structure of the HF organoid. The morphology of the lower segment-like structure of the HF organoid in cross-section is similar to that of the lower segment of the native HF and consisted of structures equivalent to the ORS, IRS, and HS, as shown in the schematic illustrations (top left). In both structures, K5, K15, CD34, and CD49f are present at the ORS. K73 is localized in the IRS, and AE13 labels the HS. The dermal papillae-specific markers (SOX2, ALP), skin-derived precursor-related marker (Nestin), and K10 are not detected. Dashed lines encircle the target structures for analysis. White arrows show the marker expression sites. All scale bars =50 μm. HF, hair follicle; HS, hair shaft; IRS, inner root sheath; ORS, outer root sheath; HE, hematoxylin-eosin.

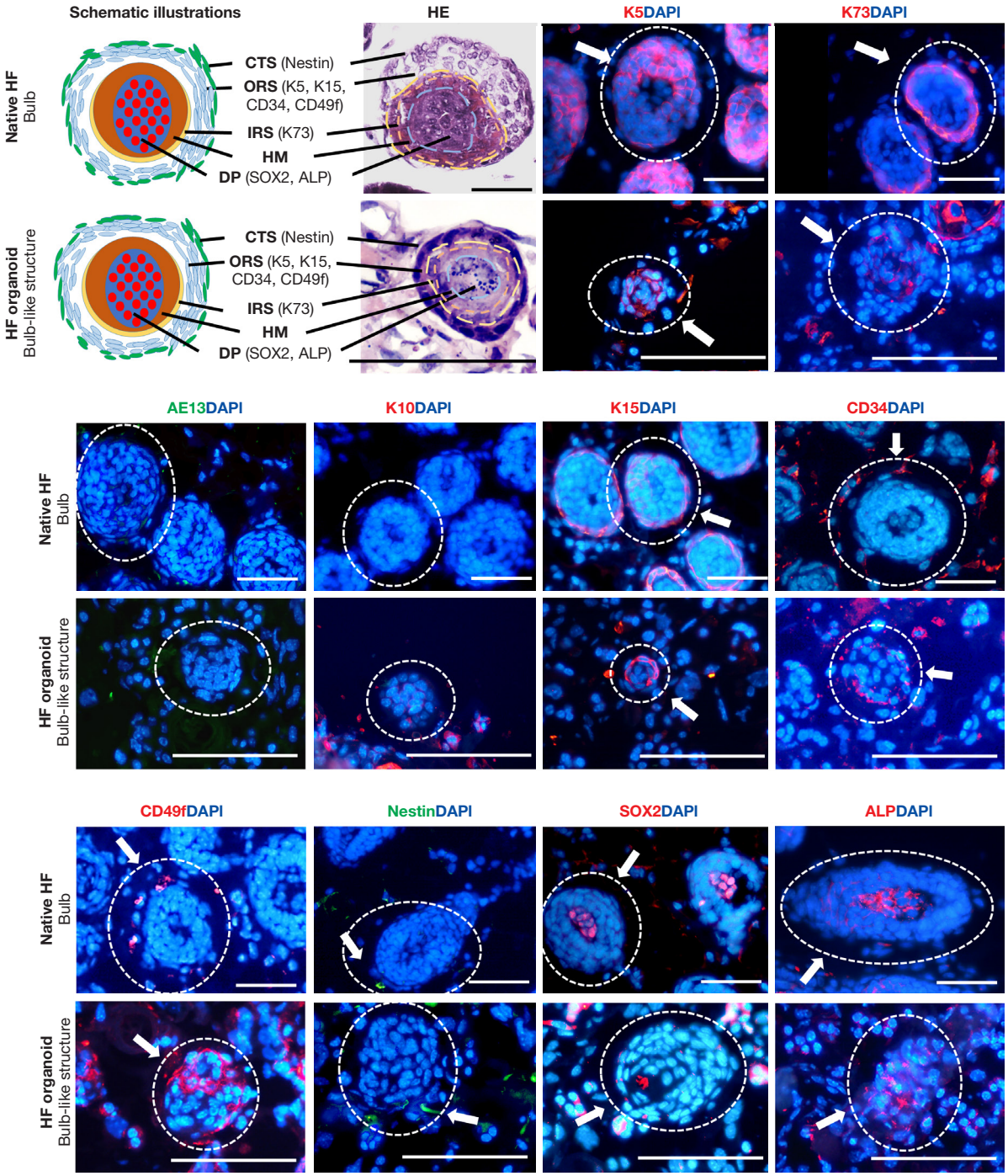

Figure 5 HE staining and expressions of HF-related markers, HF stem cell-related markers, and skin-derived precursor-related markers by IF staining in the bulb of the native HF and the bulb-like structure of the HF organoid. The morphology of the bulb-like structure of the HF organoid in cross-section is similar to that of the bulb of the native HF and consisted of structures equivalent to the CTS, ORS, IRS (in the upper bulb), HM, and DP, as shown in the schematic illustrations (top left). In both structures, K5, K15, CD34, and CD49f are present in the ORS. K73 is localized in the IRS. SOX2 and ALP are expressed in the DP. Nestin is localized in the CTS. AE13 and K10 are not detected. Dashed lines encircle the target structures for analysis. White arrows show the marker expression sites. All scale bars =50 μm. HF, hair follicle; CTS, connective tissue sheath; ORS, outer root sheath; IRS, inner root sheath; HM, hair matrix; DP, dermal papillae.

matrix, root sheath, and hair bulges (4). From the root to the tail, an HF consists of a bulb, a lower segment, and an upper segment (including the infundibulum and the isthmus). The papilla provides a reservoir of multipotent stem cells that regulate both the development and growth of the HFs (17). The bulge is located in the ORS at the insertion point of the arrector pili muscle. It houses several types of stem cells, which supply the entire HF with new cells (18). The epithelial-mesenchymal interactions of the DP and bulge play a pivotal role in hair genesis and development, regulation of periodic HF activity, and repair of injured skin (13). Therefore, the integrity of the structure is crucial to the sound function of the HF. Similarly, structural integrity plays an important role in the function and biology of HF organoids.

To judge whether the structure and function of organoids are consistent with those of native tissue, current research has compared the results of HE and the immunohistochemical expression of marker proteins in specific sites within HF organoids with those of native HF (8,9,12,14). For instance, Ataç *et al.* (13) constructed a human microfollicle (i.e., organoid) by coculture of human DP cells, ORS keratinocytes, and melanocytes in a specific medium. For the characterization, specific hair keratins' expressions were detected in the cultured aggregate, an HF bulb-like structure instead of a complete HF organoid. However, the complete structure of the HF organoid is rarely explored, especially the longitudinal structure.

A previous study found that the cuticular scales of the mouse hair shaft always pointed from the root end to the tip end (19). In our study the results confirmed that the HF organoid comprises an infundibular cyst-like structure, lower segment-like structure, and bulb-like structure. Furthermore, we showed that the various segments had a similar structure and localization of specific molecular markers to the comparable segments of native HFs. These results will help to further improve the understanding of HF organoids and provide an important research basis for the broader application of HF organoids as a model for the study of HFs.

To the best of our knowledge, this particular structure has not been reported from *in vitro* organoid studies. A similar result was reported in an *in vivo* study, called a "patch assay", by Zheng *et al.* (20). In their study, the regenerated HFs had not only the hair bulb and lower segment, but also the cyst-like structure, which was referred to as an "infundibular cyst" after intracutaneous injection of dissociated epidermal and dermal cells. They proposed that the cysts formed by the aggregation of epidermal cells, forming clusters, followed by apoptosis. Hair germs formed centrifugally from the cysts and eventually developed into mature HFs. Because the cells can move and self-organize freely by epithelial-mesenchymal interactions both in Matrigel *in vitro* and the patch assay *in vivo*, we speculate that the self-organization of HF organoids in Matrigel is similar to that of the HF formation observed by Zheng *et al.*, (20) but further studies are needed to confirm this.

In order to induce hair follicles, some growth factors will be selectively added to the medium, such as fibroblast growth factors (FGFs) and epidermal growth factor (EGF). Their roles are inconsistent. A previous study found that HF-derived organoids were found to grow best in basic medium supplemented with FGF2, and FGF10, and organoids derived from IFE could be cultured longest in basic medium supplemented with EGF, FGF10, Forskolin and transforming growth factor-β inhibitor (11). Nevertheless, EGF promoted the growth and migration of HF ORS cells in vitro, and induced bulb cell population to differentiate into an ORS phenotype. It appears that EGF targets the ORS cell growth and bulb cell differentiation more (21). Therefore, in our study, EGF was selected as the growth factor to induce HF organoids.

As HF stem cells are defined as CD49f (+)/CD34 (+) (22), we found that the ORS-like structure in all segments of the HF organoids was CD49f (+)/CD34 (+). Moreover, we observed that ALP and SOX2, specific markers of DP cells (23), localized in the DP-like structure, and Nestin was expressed in the connective tissue sheath-like structure. The Nestin-expressing stem cells from the DP have been termed skin precursors or SKP cells (24). We confirmed that the residence of HF stem cells, DP cells, and SKPs was consistent with that in the native HF. Therefore, the characteristics and function of our HF organoids were similar to native HFs. However, it should be noted that our HF organoid was self-assembled only in Matrigel. Up to now, there have been two main methods for 3D structure generation: scaffold and scaffold-free (25). Matrigel is the most common biomaterial scaffold (26). 3D droplet culture and air-liquid-interface culture are two scaffold-free techniques (27,28). Therefore, whether the structure, morphology, and function of HF organoids generated by other methods are consistent with our needs further study.

In conclusion, this study described the complete structure, morphology, and location of stem cells of HF organoids self-assembled in Matrigel, which were similar to those of native HF. In the future, we will further

explore the precise position of the bulge-like structure and the spatiotemporal process of HF organoids in their morphogenesis and maturation. We will also proceed with study from Matrigel to other methods. We believe that in the near future, the HF organoid may help elucidate novel understandings of hair health, hair loss, or regeneration, and ultimately cure hair diseases.

Acknowledgments

Funding: The study was supported in part by the National Natural Science Foundation of China (Nos. 82172231, 82172211, and 81772102).

Footnote

Reporting Checklist: The authors have completed the ARRIVE reporting checklist. Available at https://atm.amegroups.com/article/view/10.21037/atm-22-3252/rc

Data Sharing Statement: Available at https://atm.amegroups.com/article/view/10.21037/atm-22-3252/dss

Conflicts of Interest: All authors have completed the ICMJE uniform disclosure form (available at https://atm.amegroups.com/article/view/10.21037/atm-22-3252/coif). The authors have no conflicts of interest to declare.

Ethical Statement: The authors are accountable for all aspects of the work in ensuring that questions related to the accuracy or integrity of any part of the work are appropriately investigated and resolved. Experiments were performed under a project license (No. SUMC2019-217) granted by the Ethics Committee of Shantou University Medical College, in compliance with the institutional guidelines for the care and use of animals.

References

1. Ji S, Zhu Z, Sun X, et al. Functional hair follicle regeneration: an updated review. Signal Transduct Target Ther 2021;6:66.
2. Saxena N, Mok KW, Rendl M. An updated classification of hair follicle morphogenesis. Exp Dermatol 2019;28:332-44.
3. Bejaoui M, Villareal MO, Isoda H. β-catenin-mediated hair growth induction effect of 3,4,5-tri-O-caffeoylquinic acid. Aging (Albany NY) 2019;11:4216-37.
4. Schneider MR, Schmidt-Ullrich R, Paus R. The hair follicle as a dynamic miniorgan. Curr Biol 2009;19:R132-42.
5. Mishra P, Handa M, Ujjwal RR, et al. Potential of nanoparticulate based delivery systems for effective management of alopecia. Colloids Surf B Biointerfaces 2021;208:112050.
6. Wang X, Wang S, Guo B, et al. Human primary epidermal organoids enable modeling of dermatophyte infections. Cell Death Dis 2021;12:35.
7. Lei M, Schumacher LJ, Lai YC, et al. Self-organization process in newborn skin organoid formation inspires strategy to restore hair regeneration of adult cells. Proc Natl Acad Sci U S A 2017;114:E7101-10.
8. Lee J, Böscke R, Tang PC, et al. Hair Follicle Development in Mouse Pluripotent Stem Cell-Derived Skin Organoids. Cell Rep 2018;22:242-54.
9. Lee J, Rabbani CC, Gao H, et al. Hair-bearing human skin generated entirely from pluripotent stem cells. Nature 2020;582:399-404.
10. Ebner-Peking P, Krisch L, Wolf M, et al. Self-assembly of differentiated progenitor cells facilitates spheroid human skin organoid formation and planar skin regeneration. Theranostics 2021;11:8430-47.
11. Wiener DJ, Basak O, Asra P, et al. Establishment and characterization of a canine keratinocyte organoid culture system. Vet Dermatol 2018;29:375-e126.
12. Su Y, Wen J, Zhu J, et al. Pre-aggregation of scalp progenitor dermal and epidermal stem cells activates the WNT pathway and promotes hair follicle formation in in vitro and in vivo systems. Stem Cell Res Ther 2019;10:403.
13. Ataç B, Kiss FM, Lam T, et al. The microfollicle: a model of the human hair follicle for in vitro studies. In Vitro Cell Dev Biol Anim 2020;56:847-58.
14. Weber EL, Woolley TE, Yeh CY, et al. Self-organizing hair peg-like structures from dissociated skin progenitor cells: New insights for human hair follicle organoid

engineering and Turing patterning in an asymmetric morphogenetic field. Exp Dermatol 2019;28:355-66.
15. Lichti U, Anders J, Yuspa SH. Isolation and short-term culture of primary keratinocytes, hair follicle populations and dermal cells from newborn mice and keratinocytes from adult mice for in vitro analysis and for grafting to immunodeficient mice. Nat Protoc 2008;3:799-810.
16. Li H, Chen L, Zeng S, et al. Matrigel basement membrane matrix induces eccrine sweat gland cells to reconstitute sweat gland-like structures in nude mice. Exp Cell Res 2015;332:67-77.
17. Nilforoushzadeh M, Rahimi Jameh E, Jaffary F, et al. Hair Follicle Generation by Injections of Adult Human Follicular Epithelial and Dermal Papilla Cells into Nude Mice. Cell J 2017;19:259-68.
18. Shwartz Y, Gonzalez-Celeiro M, Chen CL, et al. Cell Types Promoting Goosebumps Form a Niche to Regulate Hair Follicle Stem Cells. Cell 2020;182:578-593.e19.
19. Lee E, Choi TY, Woo D, et al. Species identification key of Korean mammal hair. J Vet Med Sci 2014;76:667-75.
20. Zheng Y, Du X, Wang W, et al. Organogenesis from dissociated cells: generation of mature cycling hair follicles from skin-derived cells. J Invest Dermatol 2005;124:867-76.
21. Lin Y, Liu C, Zhan X, et al. Jagged1 and Epidermal Growth Factor Promoted Androgen-Suppressed Mouse Hair Growth In Vitro and In Vivo. Front Pharmacol 2019;10:1634.
22. Oinam L, Changarathil G, Raja E, et al. Glycome profiling by lectin microarray reveals dynamic glycan alterations during epidermal stem cell aging. Aging Cell 2020;19:e13190.
23. Kwack MH, Yang JM, Won GH, et al. Establishment and characterization of five immortalized human scalp dermal papilla cell lines. Biochem Biophys Res Commun 2018;496:346-51.
24. Uchugonova A, Duong J, Zhang N, et al. The bulge area is the origin of nestin-expressing pluripotent stem cells of the hair follicle. J Cell Biochem 2011;112:2046-50.
25. Akkerman N, Defize LH. Dawn of the organoid era: 3D tissue and organ cultures revolutionize the study of development, disease, and regeneration. Bioessays 2017. doi: 10.1002/bies.201600244.
26. Kaur S, Kaur I, Rawal P, et al. Non-matrigel scaffolds for organoid cultures. Cancer Lett 2021;504:58-66.
27. Shariati L, Esmaeili Y, Haghjooy Javanmard S, et al. Organoid technology: Current standing and future perspectives. Stem Cells 2021;39:1625-49.
28. Saleh J, Mercier B, Xi W. Bioengineering methods for organoid systems. Biol Cell 2021;113:475-91.

(English Language Editor: K. Brown)

Cite this article as: Xie S, Chen L, Zhang M, Zhang C, Li H. Self-assembled complete hair follicle organoids by coculture of neonatal mouse epidermal cells and dermal cells in Matrigel. Ann Transl Med 2022;10(14):767. doi: 10.21037/atm-22-3252